EurJIC
European Journal of Inorganic Chemistry

Full Papers
doi.org/10.1002/ejic.202100932

Chemistry Europe
European Chemical Societies Publishing

www.eurjic.org

Understanding the Binding Properties of N-heterocyclic Carbenes through BDE Matrix App

Lucía Morán-González,[a] Jaime Rodríguez-Guerra Pedregal,[a] Maria Besora,[b] and Feliu Maseras*[a]

The interaction of N-heterocyclic carbene (NHC) ligands with transition metal centers is analyzed with a set of descriptors derived from the statistical treatment of density functional theory (DFT) computational results. These descriptors, labeled as hidden descriptors (HD), had been previously defined in our group and here are applied with the help of a user-friendly web application developed for that purpose: BDE Matrix App. Five HDs are computed with little computational effort for each NHC under consideration. Expectations are confirmed in that the binding to the metal center is largely ruled by the first two descriptors, suitably associated to σ donation and π backdonation, and the approach leads to a straightforward comparison of their quantitative values. The study is extended beyond NHCs, and other neutral ligands, such as cyclopropenylidenes, phosphines, and amines are considered. The procedure is shown to be well suited to provide a unified framework for the comparison of these diverse ligands.

Introduction

N-heterocyclic carbenes (NHC) have reached a widespread use as ligands in transition metal chemistry in general and in homogeneous catalysis in particular.[1] NHCs have numerous implementations in processes such as cross-coupling,[2] olefin metathesis[3] and asymmetric catalysis.[4] In fact, in some relevant examples, such as the Grubbs catalyst,[5] they have practically replaced phosphine ligands. NHCs have been catalogued by Peris as 'Smart' ligands, because they are 'Switchable, Multifunctional, Adaptable oR Tunable'.[6]

One of the main features of these ligands are their strong and easily tunable σ donor properties. Figure 1 presents the main bonding features of the M-NHC bond. The main role is played by the σ donation from the lone pair of the ligand to a d_z^2 empty orbital of the metal (L→M), complemented by a significant π backdonation from the d_{xz} (or d_{yz}) metallic orbital to the π orbital of the ligand (L←M).[7]

The binding properties of NHCs in transition metal complexes have been the subject of a number of studies, both experimental[8] and computational.[9] Computational works have placed a particular emphasis in the application of energy and charge partitions. These studies have contributed substantially to the general understanding of the behavior of this type of ligands. The current contribution wants to complement them by an analysis based on the statistical treatment of DFT results.

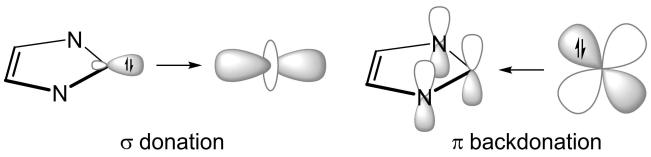

Figure 1. Most important NHC molecular orbitals (MO) involved in the NHC–M bond.

Data-led approaches open the possibility to develop statistical-based methods to provide predictions and analysis of the properties of chemicals. The use of descriptors, mathematical entities able to characterize molecules, and the relationships between them becomes crucial. The identification of such mathematical expressions requires the use of statistical tools, which cover from linear regression algorithms[10] to more cutting-edge methods such as neural networks[11] or random forest.[12]

Some descriptors have found wide use in transition metal chemistry, such as the Tolman electronic and steric parameter for phosphorus donor ligands[13] and the percent buried volume, $\%V_{buried}$, proposed to analyze the steric profile of the N-heterocyclic carbenes (NHC).[14] New descriptor-based treatments keep being developed,[15] and the current status has been recently reviewed by Durand and Fey.[16] Most descriptors under use derive directly from molecular properties, and only recently the generation of new descriptors derived from statistical treatments is gaining steam.[17]

Our group has made a contribution in this field where descriptors are no longer predefined but defined *a posteriori* through statistical treatment of a training set of structures covering a wide chemical space.[18] Our so-called hidden descriptors (HD) emerge as an alternative to describe the main

[a] *L. Morán-González, Dr. J. R.-G. Pedregal, Prof. F. Maseras*
Institute of Chemical Research of Catalonia (ICIQ),
The Barcelona Institute of Science and Technology
Avgda. Països Catalans, 16, Tarragona 43007, Catalonia, Spain
E-mail: fmaseras@iciq.es
[b] *Dr. M. Besora*
Departament de Química Física i Inorgànica,
Universitat Rovira i Virgili
c/Marcel·lí Domingo s/n, Tarragona 43007, Catalonia, Spain

Supporting information for this article is available on the WWW under https://doi.org/10.1002/ejic.202100932

Part of the "RSEQ-GEQO Prize Winners" Special Collection.

electronic features of the moieties involved in a metal-ligand bond (M–L), derived from the bond dissociation energy values (BDE). Such hidden descriptors are hierarchical and the first four of them are associated with qualitative chemical concepts: the first HD is related to the σ donation (HD_1), the second is associated to the π bonding (HD_2); the third correlates with *cis* influence (HD_3); the fourth is identified with covalency (HD_4). These HDs provide a global insight about the general capacities of each component of the M–L bond: the ligand and the metal fragment. They focus on electronic effects by design, as we considered that robust models for steric effects are already available.

A critical advantage of our scheme is that it can be easily extended to ligands outside the initial set with a low computational cost. Indeed, one needs to compute only the BDE of a given ligand with five selected metal fragments (OsO_3^{2+}, $PdH(PH_3)_2^+$, $PdPH_3$, $ZrCl_5^-$ and $InCl_2^+$) and introduce the values in a system of linear equations. We are disclosing here also an open access web application, BDE Matrix App (see Experimental Section) that uses as input the five BDEs and yields automatically the five descriptors for any given ligand.

This work uses the BDE Matrix App to analyze through the hidden descriptors emerging from our previous work a family of thirty-eight NHC-focused ligands. This provides a computationally efficient treatment for the characterization of their properties and their placement among the overall scheme of related ligands.

Results and Discussion

We first study the twenty two NHC ligands presented in Figure 2, covering the most common types of NHCs. For the sake of clarity, NHC are labeled following the criteria defined by Gusev.[9b] The nomenclature follows the scheme [parentheterocycle](substituents)$_n$N(substituents)$_m$. The parent heterocycles chosen are imidazole (Im), imidazoline (sIm), pyrazole (Pyraz), abnormal-imidazole (aIm), triazole (Triaz), pyridine (PyC4), saturated pyrimidine (sPm), benzimidazole (BIm) and dipyridoimidazole (DPyIm); and as substituents, there are alkyl (Me, Et, ^{i}Pr), aryl (Ph), F, CN, NO_2 and NMe_2 groups. NHC are highly modular, thus leading to a broad diversity of species.

We will also group at certain points the ligands in families: normal NHC (nNHC), which contain the imidazole, imidazolidine and triazole cores; reduced heteroatom stabilized, which are of the PyrazC3NR_2 type; cyclic(alkyl)(amino)carbenes (CAAC) and remote ligands (rNHC), involving pyridine-derived structures and abnormal NHC (aNHC). All the ligands considered have a singlet ground state. A similar analysis could be carried out on carbene ligands in the triplet state, but this is not the focus of the present work.

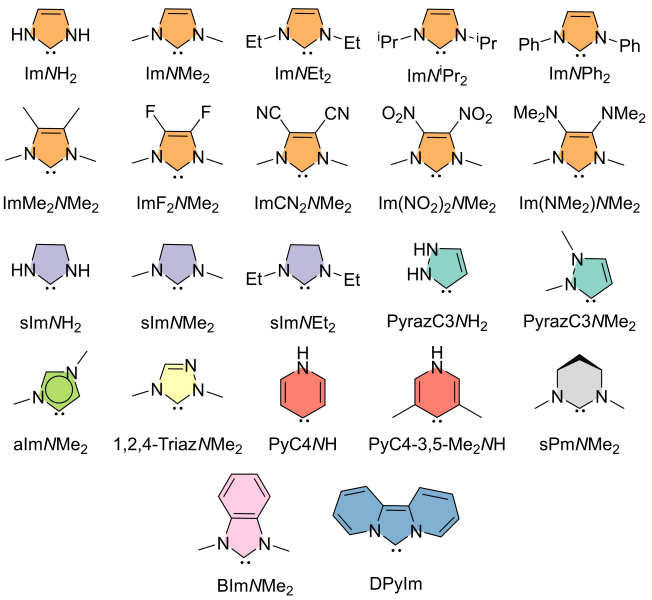

Figure 2. NHC structures. Colors: orange: imidazole (Im); violet: imidazoline (sIm); turquoise: pyrazole (Pyraz); lime green: abnormal-imidazole (aIm); yellow: triazole (Triaz); red: pyridine (PyC4); grey: saturated pyrimidine (sPm); pink: benzimidazole (BIm) and blue: dipyridoimidazole (DPyIm).

Hidden descriptor identification and meaning

We applied the hidden descriptor strategy as explained in the Experimental Section and in the Supporting Information. All the computed BDEs between each metal fragment of reference and ligands are reported in the SI. The resulting hidden descriptors for each of the ligands in Figure 2, which we will refer as HDL, are reported in Table 1.

Table 1. Hidden descriptor values of NHC ligands.

NHC ligands	HDL_1	HDL_2	HDL_3	HDL_4	HDL_5
Im*N*H_2	0.193	−0.160	−0.123	0.038	−0.092
ImNMe_2	0.200	−0.220	−0.038	−0.025	−0.089
Im*N*Et_2	0.204	−0.243	−0.080	−0.032	−0.047
Im*N*^{i}Pr_2	0.207	−0.243	−0.105	−0.030	−0.034
Im*N*Ph_2	0.204	−0.295	0.011	−0.145	−0.079
Im$(NO_2)_2$*N*Me_2	0.151	−0.270	−0.117	0.068	−0.101
ImCN_2*N*Me_2	0.162	−0.259	−0.106	0.040	−0.089
ImF_2*N*Me_2	0.185	−0.227	−0.039	−0.020	−0.131
ImMe_2*N*Me_2	0.210	−0.220	0.005	−0.082	−0.123
Im(NMe_2)*N*Me_2	0.227	−0.188	0.197	−0.269	−0.378
sIm*N*H_2	0.190	−0.192	−0.185	0.046	−0.027
sIm*N*Me_2	0.194	−0.269	−0.091	−0.043	−0.029
sIm*N*Et_2	0.197	−0.285	−0.123	−0.028	0.019
PyrazC3*N*H_2	0.210	−0.174	−0.114	0.004	0.004
PyrazC3*N*Me_2	0.219	−0.185	−0.101	0.009	0.036
sPm*N*Me_2	0.192	−0.320	0.025	−0.082	0.043
PyC4*N*H	0.238	−0.175	−0.136	−0.021	0.028
PyC4-3,5-Me_2*N*H	0.239	−0.292	−0.011	−0.117	0.081
BIm*N*Me_2	0.193	−0.245	−0.037	−0.050	−0.115
DPyIm	0.219	−0.155	0.135	−0.197	−0.372
aIm*N*Me_2	0.230	−0.159	−0.064	0.001	0.009
1,2,4-Triaz*N*Me_2	0.180	−0.237	−0.144	0.028	−0.044

A first inspection shows the results are reasonable. The positive HDL_1 sign involves σ donor ability and the negative HDL_2 sign implies π acceptor behaviour. This is what should be expected, and will be discussed in the following section.

We can also examine the average weight of each descriptor in the BDE of this current set (CS) of NHC and compare it with the average weight in the general set (initial study, IS).[18] The results are summarized in Table 2. The procedure to compute the %weight (CS) is reported in the SI.

The first two hidden descriptors already accounted for 84.7% of the total BDE for the initial study set, and their relative weight increases further to 95.7% in the current set of NHC. The binding ability of these ligands can be thus well characterized by these two descriptors, associated to σ donor and π acceptor properties. Contributions from *cis* effects and bond covalency are much smaller.

HD Analysis for Selected NHCs

We analyze here what the HDs say about the relevant features of the ligands: the σ donation and the π acceptance. The maximum value of HDL_1 is 0.239, which corresponds to a 6-membered cycle, PyC4-3,5-Me_2*N*H, and the strongest σ donor of the five-membered cycles is aImNMe_2 with HDL_1 value of 0.230. This trend was expected, as they are a CAAC and an abnormal NHC.[19]

The lowest value, 0.151, for HDL_1 corresponds to Im-$(NO_2)_2NMe_2$, and can be explained by the presence of an NO_2 substituent, which is the most electron-withdrawing group in the set of ligands under consideration. For HDL_2, the extreme values are −0.155 for DPyIm and −0.320 for sPmNMe_2. When looking at the structures, we notice that DPyIm presents a high aromaticity and delocalization, while the behaviour is opposite for sPmNMe_2, which is fully saturated except for the carbene group.

Some trends can be also observed from the values for HDL_1 and HDL_2 reported in Table 1:

(i) unsaturated carbenes (ImNR_2 R = H, Me, Et) are stronger σ donors and weaker π acceptors than their saturated analogues (sImNR_2 R = H, Me, Et).

(ii) the length of the chain in the substituents on the nitrogen atoms enhance both σ donating and π accepting properties. Both abilities increase in the order H < Me < Et < ^{i}Pr for ImNR_2 and sImNR_2 cores, and there also the couples Pyc4NH < Pyc4-3,5-Me_2NH, and PyrazC3NH_2 < PyrazC3NMe_2.

(iii) substituents on C4 and C5 positions in five-member rings affect mostly the σ donating ability of the ligand. Electron-withdrawing groups decrease it, and the electron-donating groups increase it. We see this in the variation of HDL_1 (R = NO_2 < CN < F < H < Me < NMe_2) with the series of ligands ImR_2NMe_2.

(iv) CAACs and abnormal NHC ligands are stronger σ donors than their corresponding normal NHC counterparts.

These trends follow the expectations and had been already discussed in part by other authors.[20] But it is nice to see that they appear naturally upon the straightforward application of our hidden descriptor treatment.

Table 2. Hidden descriptor % weights for the ligands in the initial study (% Weight (IS)) and in the current set (% Weight (CS)).

HD	[%] Weight (IS)	[%] Weight (CS)
1	74.7	78.7
2	10.0	17.0
3	4.2	2.5
4	3.4	0.6
5	2.3	1.1

Hidden Descriptors *vs* Conventional Descriptors

We have just shown how the hidden descriptors provide a satisfactory description of the bonding between NHC and metal fragments. We will now examine if this can be accomplished in a similar way with other descriptors of widespread use which may be even easier to compute. For this, we have first to quantify with a single number the binding ability of each descriptor. We used for this purpose the calculations already available from the use of BDE Matrix App. We had computed the binding energy in water between each ligand and five specific metal fragments (OsO_3^{2+}, $PdH(PH_3)_2^+$, $PdPH_3$, $ZrCl_5^-$ and $InCl_2^+$), which were found in our previous work to be representatively diverse. We use now these five values to calculate the arithmetic average $\overline{BDE_i}$ associated to each ligand, and we will use this as an estimation of its binding efficiency.

The binding of NHC to metal fragments is generally accepted to be mainly governed by σ donation, which has been confirmed by our analysis above. Thus, we would expect a good correlation between descriptors usually associated to σ donation and the BDE of NHC to metal fragments. We evaluated the performance of several standard descriptors usually associated with σ donor behaviour. The first of them was the energy of the highest occupied molecular orbital (E_{HOMO}) of the ligand. We examined the correlation between E_{HOMO} and finding a poor r^2 value of 0.723, the results are plotted as blue dots in Figure 3. We tried to refine the E_{HOMO} value by replacing the orbitals with the wrong symmetry ($E_{\sigma\text{-}HOMO}$, black dots in Figure 3), and we also tried to use the energy supplied by Natural Bond Orbital (NBO) analysis for the lone pair located in the carbene carbon ($E_{LP(C)}$, pink dots in Figure 3). The correlations were in these two cases even lower, which was clearly underwhelming.

There is a simple qualitative explanation to this failure of orbital-related parameters. The molecular orbital associated to the carbene lone pair has always a minor contribution from the mixing of atomic orbitals away from the carbon center, and the size of this contribution depends on the specific characteristics of each NHC. In fact, if we analyzed the plots in more detail, we could see some subsets with good correlation, that would correspond to related groups of ligands, where the mixing of orbitals is similar. We are sure that methods can be applied to obtain a more efficient estimation of the binding ability from

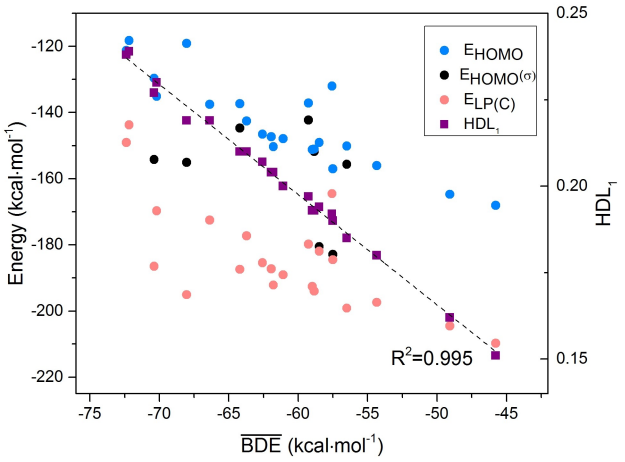

Figure 3. Left axis: BDE of each ligand versus the values of the HOMO energy ($R^2 = 0.723$), the σ-HOMO energy ($R^2 = 0.400$) and the NBO energy of the LP localized in the carbon atom ($R^2 = 0.504$). Right axis: $\overline{BDE_i}$ of each ligand versus the HDL_1 ($R^2 = 0.995$).

the HOMO, but they would hardly be able to compete in terms of simplicity and computer effort with our hidden descriptor approach. And the results of the hidden descriptor approach, also shown in Figure 3 (HD_{L1}, purple dots) are excellent. The correlation with $\overline{BDE_i}$ is in this case as high as 0.995.

We expect E_{HOMO} to be a good descriptor for other ligands, and we think that this is just an unfortunate case. But it is worth emphasizing that HDL_1 seems to be free from this defective behavior.

We could carry out a similar discussion to that presented above on the second hidden descriptor, HDL_2, related to π effects. However, we are omitting it because the choice for conventional descriptors is less intuitive, and the overall energies involved are intrinsically smaller.

Extended Set

Hidden descriptors do not only rationalize the electronic role of a single type of ligands, but they are also useful to compare any type of ligand regardless of their nature. In this concern, we have analysed the set of eight cyclopropenylidenes (CP), six phosphines (PR'_3) and two amines (NR''_3) represented in Figure 4. We selected them because of their usefulness and their similarity with NHC ligands (*e.g.* NHC ligands had initially been viewed as 'phosphine mimics' and CPs are also carbocyclic carbenes).

The full set of ligands considered, CP, PR'_3, NR''_3, and NHC, are all neutral, σ donor and π acceptor. The goal here is to see to which extent the HD treatment is able to discriminate between them. The HD values for all the ligands are gathered in the SI. Figure 5 presents a scatter plot of HDL_1 and HDL_2 values of the whole set of ligands of this work.

It is clear that the different families of ligands have diverging properties. NHCs are in general stronger σ donors than phosphines, as has been widely reported in the

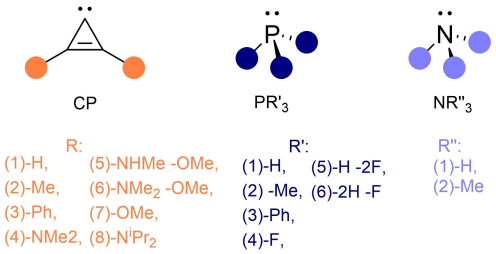

Figure 4. Cyclopropenylidenes (CP), phosphines (PR'_3) and amines (NR''_3) used in this study.

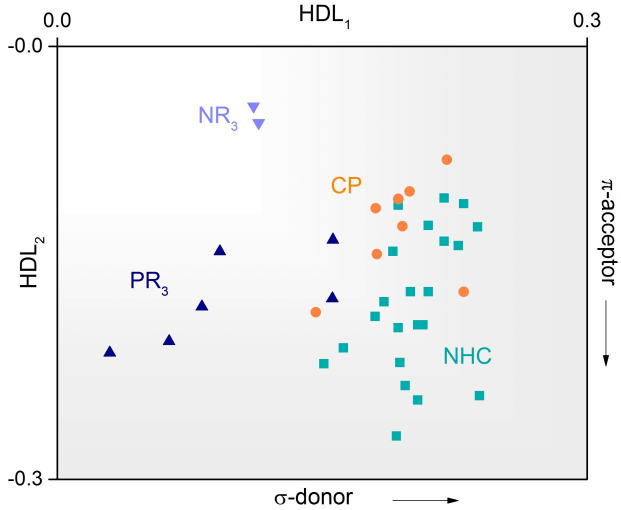

Figure 5. Scatter plot of HDL_1 and HDL_2 for the 38 ligands.

literature.[7,21] They present a wide range of π-accepting abilities, but they can also reach higher values than phosphines. CPs have a significant overlap with NHCs. They bear similar donation properties, but CPs are in general less π acceptor than NHCs. The two amines we tested overlap with the phosphines in terms of σ donation, but are clearly the weakest π acceptors.

Conclusion

The application of the hidden descriptor treatment, through the BDE Matrix App, to twenty two different NHC ligands leads to a straightforward quantitative evaluation of their σ donating and π accepting abilities in transition metal complexes. The overall behavior of the ligands follows generally expected trends, and the detailed analysis allows an in-depth understanding of their differences. These conceptually simple and easy-to-compute hidden descriptors are shown to provide a more efficient analysis than other more common descriptors for σ donation such as HOMO energies. The extension of the same type of analysis to other species such as cyclopropenylidenes, phosphines and amines is straightforward, and yields information on the differences between these related families of ligands.

Experimental Section

Energy calculations

The computational method for calculation of energies follows the specifications of the hidden descriptors treatment for BDE in transition metal complexes. All electronic structure calculations were carried out with the Gaussian 09[22] program using DFT. The pyssian library[23] was used for generation of input files. The geometries were optimized with the B3LYP-D3 functional, where empirical dispersion was added by means of Grimme's dispersion correction.[24] The 6-31 + G(d)[25] was used for elements between H and Cl, and Stuttgart/Dresden effective core potential (ECP), together with the corresponding SDD basis set for the heavier atoms. In order to simulate the solvent, single-point calculations on the B3LYP-D3 optimization structures were computed in water using polarizable continuum model (PCM).[26] Harmonic vibrational frequencies were computed on the geometry optimization level to ensure the nature as true minima of the species. All energies reported correspond to the potential energies in the water phase plus zero-point energy corrections (ZPE) from the vacuum calculations. Natural Bond Orbital (NBO)[27] calculations were also carried out. A data set collection of computational results is available in the ioChem-BD repository,[28] and is accessible via https://dx.doi.org/10.19061/iochem-bd-1-220.

BDE Matrix App.

The five hidden descriptors for each of the ligands were obtained through the web application BDE Matrix App, developed in our group, and publicly accessible in https://maserasgroup-repo.github.io/bdeapp/. BDE Matrix App uses as input the BDE energies of a given target ligand with five selected metal fragments and yields as output the five hidden descriptors for this ligand. For this work, we were interested in values in water, considered more informative, which uses as reference metal fragments $InCl_2^+$, OsO_3^{2+}, $PdPH_3$, $PdH(PH_3)^{2+}$ and $ZrCl_5^-$. Upon introduction of the five BDE values as input for one ligand (L), the corresponding descriptors are generated by solving the following system of equations:

$$HDL_k = \sum_{ref=1}^{5} \alpha_{k,ref} \cdot BDE_{ref,L} + \beta_k$$

The parameters $\alpha_{k,ref}$ and β_k are implemented in the application for each HD_k. They were obtained in our previous publication.[18] Only three of the ligands used in the current work were considered in the previous publication $ImNH_2$, PH_3 and NH_3. Thus, no singular value decomposition (SVD) analysis is carried on the results being currently reported. Further details on the web application are given in the Supporting Information.

Acknowledgements

We thank Raúl Pérez-Soto for technical support with the web application. We acknowledge financial support from the CERCA Programme/Generalitat de Catalunya, MCIN/AEI (PGC2018-100780-B-I00, PID2020-112825RB-I00 and CEX2019-000925-S) and FEDER funds. L.M.-G. thanks Generalitat de Catalunya for a FI-Agaur predoctoral contract, 2020FI-B 00245.

Conflict of Interest

The authors declare no conflict of interest.

Keywords: Bond dissociation energy · Density functional calculations · Hidden descriptors · Metal-ligand bond · N-heterocyclic carbenes

[1] a) S. Díez-González, S. P. Nolan, *Coord. Chem. Rev.* **2007**, *251*, 874–883; b) V. A. Voloshkin, N. V. Tzouras, S. P. Nolan, *Dalton Trans.* **2021**, *50*, 12058–12068; c) P. Bellotti, M. Koy, M. N. Hopkinson, F. Glorius, *Nat. Rev. Chem.* **2021**, *5*, 711–725.
[2] a) Y.-C. Hsu, V. C.-C. Wang, K.-C. Au-Yeung, C.-Y. Tsai, C.-C. Chang, B.-C. Lin, Y.-T. Chan, C.-P. Hsu, G. P. A. Yap, T. Jurca, T.-G. Ong, *Angew. Chem. Int. Ed.* **2018**, *57*, 4622–4626; *Angew. Chem.* **2018**, *130*, 4712–4716; b) H. Ohmiya, *ACS Catal.* **2020**, *10*, 6862–6869.
[3] a) G. C. Vougioukalakis, R. H. Grubbs, *Chem. Rev.* **2010**, *110*, 1746–1787; b) O. M. Ogba, N. C. Warner, D. J. O'Leary, R. H. Grubbs, *Chem. Soc. Rev.* **2018**, *47*, 4510–4544.
[4] a) R. K. M. Khan, S. Torker, A. H. Hoveyda, *J. Am. Chem. Soc.* **2013**, *135*, 10258–10261; b) K. Zhao, D. Enders, *Angew. Chem. Int. Ed.* **2017**, *56*, 3754–3756; *Angew. Chem.* **2017**, *129*, 3808–3810.
[5] a) M. Scholl, S. Ding, C. W. Lee, R. H. Grubbs, *Org. Lett.* **1999**, *1*, 953–956; b) J. Huang, E. D. Stevens, S. P. Nolan, J. L. Petersen, *J. Am. Chem. Soc.* **1999**, *121*, 2674–267.
[6] E. Peris, *Chem. Rev.* **2018**, *118*, 9988–10031.
[7] M. N. Hopkinson, C. Richter, M. Schedler, F. Glorius, *Nature* **2014**, *510*, 485–496.
[8] H. V. Huynh, *Chem. Rev.* **2018**, *118*, 9457–9492.
[9] a) G. Heydenrych, M. von Hopffgarten, E. Stander, O. Schuster, F. Helgard, H. G. Raubenheimer, G. Frenking, *Eur. J. Inorg. Chem.* **2009**, 1892–1904; b) D. G. Gusev, *Organometallics* **2009**, *28*, 6458–6461; c) N. S. Antonova, J. J. Carbó, J. M. Poblet, *Organometallics* **2009**, *28*, 4283–4287; d) L. M. Azofra, S. V. C. Vummaleti, Z. Zhang, A. Poater, L. Cavallo, *Organometallics* **2020**, *39*, 3972–3982.
[10] a) S. Aguado-Ullate, M. Urbano-Cuadrado, I. Villalba, E. Pires, J. I. García, C. Bo, J. J. Carbó, *Chem. A Eur. J.* **2012**, *18*, 14026–14036; b) S. Zhao, T. Gensch, B. Murray, Z. L. Niemeyer, M. S. Sigman, M. R. Biscoe, *Science* **2018**, *362*, 670–674.
[11] a) J. P. Janet, S. Ramesh, C. Duan, H. J. Kulik, *ACS Cent. Sci.* **2020**, *6*, 513–524; b) P. Friederich, G. Dos Passos Gomes, R. De Bin, A. Aspuru-Guzik, D. Balcells, *Chem. Sci.* **2020**, *11*, 4584–4601.
[12] a) D. T. Ahneman, J. G. Estrada, S. Lin, S. D. Dreher, A. G. Doyle, *Science* **2018**, *360*, 186–190; b) S. M. Maley, D. H. Kwon, N. Rollins, J. C. Stanley, O. L. Sydora, S. M. Bischof, D. H. Ess, *Chem. Sci.* **2020**, *11*, 9665–9674.
[13] C. A. Tolman, *J. Am. Chem. Soc.* **1970**, *92*, 2956–2965.
[14] A. Poater, B. Cosenza, A. Correa, S. Giudice, F. Ragone, V. Scarano, L. Cavallo, *Eur. J. Inorg. Chem.* **2009**, 1759–1766.
[15] a) L. Falivene, Z. Cao, A. Petta, L. Serra, A. Poater, R. Oliva, V. Scarano, L. Cavallo, *Nat. Chem.* **2019**, *11*, 872–879; b) M. Besora, A. Olmos, R. Gava, B. Noverges, G. Asensio, A. Caballero, F. Maseras, P. J. Pérez, *Angew. Chem. Int. Ed.* **2020**, *59*, 3112–3116; *Angew. Chem.* **2020**, *132*, 3136–3140.
[16] D. J. Durand, N. Fey, *Chem. Rev.* **2019**, *119*, 6561–6594.
[17] a) N. Fey, A. Koumi, A. V. Malkov, J. D. Moseley, B. N. Nguyen, S. N. G. Tyler, C. E. Willans, *Dalton Trans.* **2020**, *49*, 8169–8178; b) A. I. Green, C. P. Tinworth, S. Warriner, A. Nelson, N. Fey, *Chem. Eur. J.* **2021**, *27*, 2402–2409.
[18] O. Lakuntza, M. Besora, F. Maseras, *Inorg. Chem.* **2018**, *57*, 14660–14670.
[19] O. Schuster, L. Yang, H. G. Raubenheimer, M. Albrecht, *Chem. Rev.* **2009**, *109*, 3445–3478.
[20] a) R. A. Kely III, H. Clavier, S. Giudice, N. M. Scott, E. D. Stevens, J. Bordner, I. Samardjiev, C. D. Hoff, L. Cavallo, S. P. Nolan, *Organometallics* **2008**, *27*, 202–210; b) A. Fürstner, M. Alcarazo, K. Radkowski, C. W. Lehmann, *Angew. Chem. Int. Ed.* **2008**, *47*, 8302–8306; *Angew. Chem.* **2008**, *120*, 8426–8430.
[21] J. Huang, H. J. Schanz, E. D. Stevens, S. P. Nolan, *Organometallics* **1999**, *18*, 2370–2375.
[22] *Gaussian 09, Revision D.01*, M. J. Frisch, G. W. Trucks, H. B. Schlegel, G. E. Scuseria, M. A. Robb, J. R. Cheeseman, G. Scalmani, V. Barone, G. A. Petersson, H. Nakatsuji, X. Li, M. Caricato, A. Marenich, J. Bloino, B. G.

Janesko, R. Gomperts, B. Mennucci, H. P. Hratchian, J. V. Ortiz, A. F. Izmaylov, J. L. Sonnenberg, D. Williams-Young, F. Ding, F. Lipparini, F. Egidi, J. Goings, B. Peng, A. Petrone, T. Henderson, D. Ranasinghe, V. G. Zakrzewski, J. Gao, N. Rega, G. Zheng, W. Liang, M. Hada, M. Ehara, K. Toyota, R. Fukuda, J. Hasegawa, M. Ishida, T. Nakajima, Y. Honda, O. Kitao, H. Nakai, T. Vreven, K. Throssell, J. A. Montgomery, Jr., J. E. Peralta, F. Ogliaro, M. Bearpark, J. J. Heyd, E. Brothers, K. N. Kudin, V. N. Staroverov, T. Keith, R. Kobayashi, J. Normand, K. Raghavachari, A. Rendell, J. C. Burant, S. S. Iyengar, J. Tomasi, M. Cossi, J. M. Millam, M. Klene, C. Adamo, R. Cammi, J. W. Ochterski, R. L. Martin, K. Morokuma, O. Farkas, J. B. Foresman, D. J. Fox, Gaussian, Inc., Wallingford CT, **2016**.

[23] R. Pérez-Soto, M. Besora, F. Maseras, *pyssian v1.0.2*, Maseras Lab, July 1, **2021**, URL: https://doi.org/10.5281/zenodo.5055860.

[24] a) A. D. Becke, *J. Chem. Phys.* **1993**, *98*, 5648–5652; b) C. Lee, W. Yang, R. G. Parr, *Phys. Rev. B* **1988**, *37*, 785–789; c) S. Grimme, J. Antony, S. Ehrlich, H. Krieg, *J. Chem. Phys.* **2010**, *132*, 15410.

[25] a) G. A. Petersson, A. Bennett, T. G. Tensfeldt, M. A. Al-Laham, W. A. Shirley, J. Mantzaris, *J. Chem. Phys.* **1988**, *89*, 2193–2218; b) G. A. Petersson, M. A. Al-Laham, *J. Chem. Phys.* **1991**, *9*, 6081–6090.

[26] a) J. Tomasi, B. Mennucci, R. Cammi, *Chem. Rev.* **2005**, *105*, 2999–3094; b) G. Scalmani, M. J. Frisch, *J. Chem. Phys.* **2010**, 132.

[27] *NBO Version 6.0*, E. D. Glendening, J. K. Badenhoop, A. E. Reed, J. E. Carpenter, J. A. Bohmann, C. M. Morales, C. R. Landis, F. Weinhold, NBO 6.0, Theoretical Chemistry Institute, University of Wisconsin, Madison, **2013**.

[28] M. Álvarez-Moreno, C. De Graaf, N. López, F. Maseras, J. M. Poblet, C. Bo, *J. Chem. Inf. Model.* **2015**, *55*, 95–103.

Manuscript received: October 28, 2021
Revised manuscript received: November 24, 2021
Accepted manuscript online: November 29, 2021